NUMERICAL STUDY OF INTERVERTEBRAL PROSTHESIS

A. PÉREZ[*], I. ALIGUER[*], C.M. LÓPEZ[*], I. CAROL[*] and A. MOLINA[*][†]

[*] Department of Geotechnical Engineering and Geo-Sciences
Universidad Politécnica de Cataluña
Jordi Girona 1, Edif. D2, E-08034 Barcelona, Spain
e-mail: adria.perez@upc.edu, ignasi.aliguer@upc.edu, carlos.maria.lopez@upc.edu, ignacio.carol@upc.edu

[†] Service of Traumatology and Orthopedics, Raquis Section
Hospital del Mar, Municipal Institute of Health Care of Barcelona (I.M.A.S.)
Paseo Marítimo 25-29, 08003 Barcelona, Spain
e-mail: amolina@parcdesalutmar.cat

Key words: Finite element analysis, Lumbar interbody fusion, Frictional mechanisms.

Abstract. Lumbar interbody fusion is a lumbar surgical procedure that consists of replacing the intervertebral disk with a stiff prosthetic device (the fusion cage), with the purpose of promoting bone growth in between the two vertebrae and finally fuse them into one single rigid unit. The numerical studies described in this paper are oriented to clarify the mechanical behavior of the new vertebral configuration after the fusion cage has been installed. The geometrical model includes vertebrae L5 and S1 and has been directly generated from radiological images, with individual representation of the stiffer cortical bone on the surface and the softer trabecular bone in the interior, as well as two kinds of prosthesis devices in between the two vertebrae. The resulting stresses are discussed on the basis of a hyperbolic Mohr-Coulomb failure criterion in comparison to traditional von Mises.

1 INTRODUCTION

Lumbar interbody fusion is a lumbar surgical procedure that consists of replacing the intervertebral disk with a stiff prosthetic device (the fusion cage), promote bone growth in between the two vertebrae, and finally fuse them into one single rigid unit. The fusion cage is usually hollow to be able to accommodate new bone in its interior. Often this kind of surgery has been considered the only option when disk diseases are severe.

On the market there are many different types of cages available that have been applied as prosthesis. The main variants between different types of cages are the material (titanium, carbon, polymer), the shape (square, rectangular, cylindrical) and the contact surface with the endplate (smooth, rough, with ridges). In literature there are many publications comparing various types of cages [1-5].

In relation to the numerical simulation of the mechanical behavior, there are several publications about specific modeling of the lumbar area using the finite element method (FEM) [6, 7].

There are various models that analyze the intervertebral disc of vertebral segments [8, 9] and various studies that include fusion cages in the modeling [10, 11, 12]. In most of these models the results are presented in terms of the so-called von Mises stress, which summarizes with a single scalar value the (actually multi-component) stress state at a point. This magnitude in fact only represents the deviatoric stresses, while some studies [13] show that the behavior of cortical bone is actually dependent on the hydrostatic pressure (I_1 invariant) as well, and it also exhibits additional frictional mechanisms. In frictional materials the hydrostatic pressure has an important influence on the strength of the material. Therefore, to represent stress states of the cortical tissue, it seems more appropriate to use an equivalent stress criterion or a more appropriate strength surface for the frictional behavior.

This paper summarizes some of the numerical results obtained with a three-dimensional model of a vertebral segment, developed by the authors as described briefly in the next section. The continuum stress results are discussed using a Mohr-Coulomb hyperbolic model type (Hyperbolic Mohr-Coulomb Model) in comparison to traditional von Mises.

2 MATERIALS AND METHODS

The geometry and three-dimensional mesh of the vertebral segment formed by the last lumbar (L5) and the first sacral (S1) vertebrae have been generated. Two types of prosthesis (cages) of similar design and different material are incorporated into the model, one of P.E.E.K polymer and the other of metallic alloy (Ti6AQ14V).

2.1 Generation of the Geometry

First, using the Mimics program a closed surface of each vertebra were obtained from CT images of a patient (CAT scan), which led to the generation of a three-dimensional model of the vertebra. These images were processed with other programs (Femap 8.3, Rhinoceros 3D) until a suitable geometry was obtained. Because the complete modeling of both vertebrae represented a very large number of degrees of freedom for the modeling, and given the symmetry of the problem only half of each vertebrae was considered in the discretization. In order to differentiate the cortical bone layer from the trabecular bone core an extrusion towards the inside of the original surface was performed with a thickness of 0.6 mm.

On the other hand, the geometry of both prosthesis (cages) was generated from actual samples by using computer graphics programs. A simplified design of the Sherpa fixing system adapted to the size of the represented vertebrae has also been generated.

This original geometry of the vertebral set was used to generate a mesh of linear tetrahedrons, with which preliminary numerical studies were carried out and led to evidence that the shell behavior of cortical bone is the one that governs the problem.

For this reason a new approach using prismatic elements of triangular base in the area of cortical bone was used. Prisms of triangular base were generated by an extrusion process of the external surface of the trabecular tissue.

2.2 Generation of the FEM mesh

The FE analysis was first performed using a tetrahedral mesh and looking at the results in terms of conventional continuum stresses. A second study took advantage of the fact that cortical bone seems to work as a bending shell. Based on that, a new mesh was developed with the cortical represented by extruded prismatic elements of triangular base, in such way that all integration points through the thickness were aligned and it became possible to calculate the shell forces (moment, shear and axial) associated to the cross-sectional behavior of the cortical shell.

Figure 1 shows the overall mesh generated with quadratic elements for each type of prosthesis, and Table 1 summarizes some statistics of these meshes.
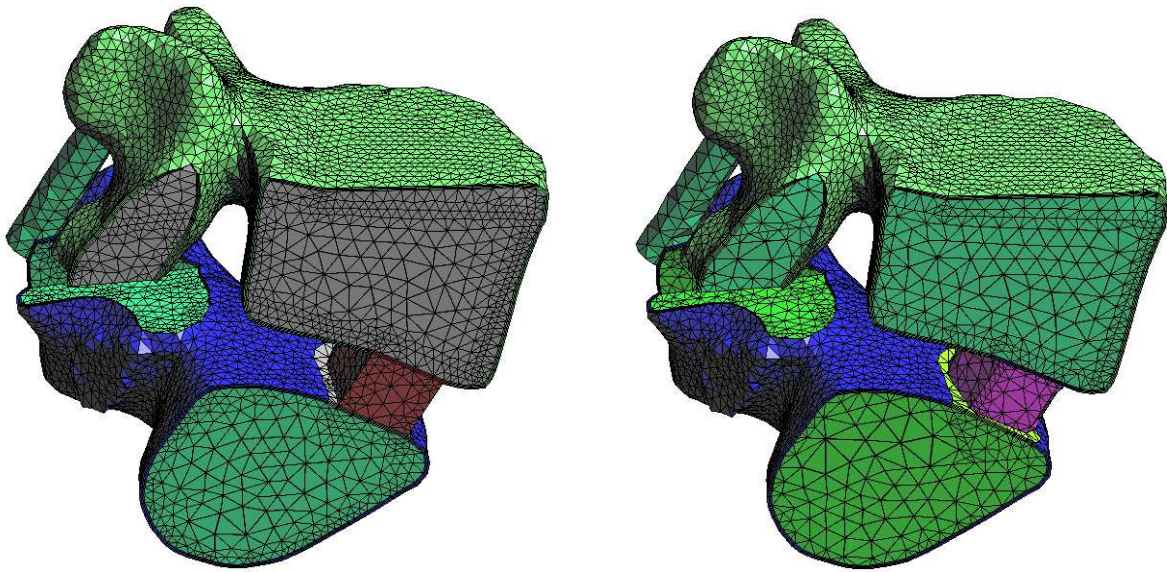
Figure 1: FEM mesh of the model with polymer prosthesis (left), and metallic alloy prosthesis (right).

2.3 Boundary and loading conditions

The displacements of the lateral-bottom side of the S1 vertebra are prevented, simulating the contact with the pelvis. Furthermore, conditions of symmetry are applied (displacements perpendicular to the symmetry plane are prevented on the same, $x = 0$).

The procedure described in [8] has been followed to define the loads to be applied. A normal compression load state has been assumed, where a preload of 1000 N simulates vertical rest position of the column, and a load of 4000 N (2000N on the "semi-vertebra").

	Number of nodes	Number of elements	Number of PRSM	Number of TETR
Polymer model	161488	76130	36579	39551
Metallic alloy model	146380	65699	36390	29309

Table 1: Statistics for each of the two meshes analyzed.

2.4 Material failure criterion

In the biomechanical literature it seems traditional to represent the stress state by means of the equivalent von Mises stress [10]. However, some studies [13] show that the behavior of cortical bone is dependent on the hydrostatic pressure (I_1 invariant) as well, and also exhibits additional frictional mechanisms. In this paper the continuum stress results are discussed using a hyperbolic Mohr-Coulomb model (HMCM) in comparison to traditional von Mises.
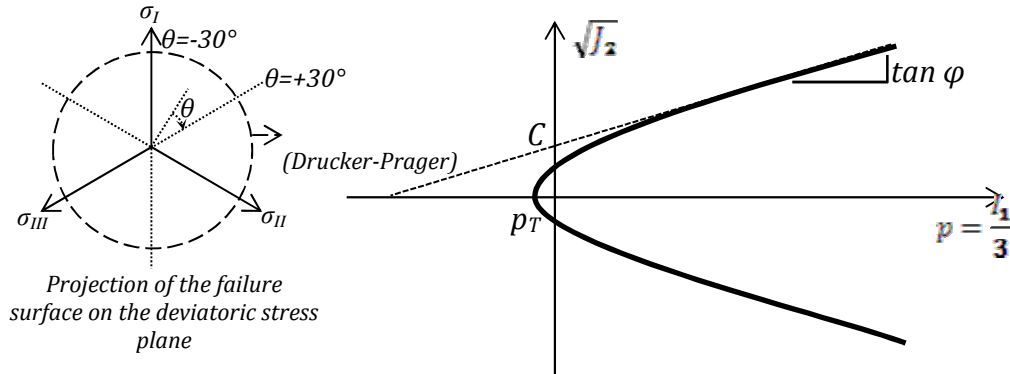

Figure 2: HMCM strength surface.

The von Mises stress provides the essential ingredient for immediate verification of the von-Mises criterion, which depends on a single parameter, the octahedral shear strength. It only takes into account the influence of the second invariant of the deviatoric stress tensor (J_2), neglecting the influence of the first invariant of the stress tensor (I_1).

The Mohr-type failure criteria in general, and in particular the HMC criterion is based on the model originally proposed in [14, 15] for zero-thickness interface elements, whose formulation was later adapted for the continuum medium. This failure criterion is defined by a hyperboloid defined by three parameters (Figure 2): the triaxial tensile strength (p_T), the apparent cohesion (C) and the slope of the conical surface in the $p - \sqrt{J_2}$ space (tan φ). This criterion may be expressed in the following way:

$$F(I_1, J_2) = \sqrt{J_2 + (C - p_T \tan \varphi)^2} - \left(C - \frac{I_1}{3} \tan \varphi\right) = 0 \qquad (1)$$

3 NUMERICAL RESULTS

The calculations have been performed assuming linear elastic behavior of the material, using the parameters presented in Table 2.

Figure 3 shows the stress distribution in the cortical and trabecular tissue (left to right) in a cross-section of the cortical bone and nearby trabecular bone, near the symmetry plane located below the prosthesis in the vertebra S1. The stress represented is σ_3 for those Gauss points at which compression is predominant, and σ_1 for those at which tensile stress is

predominant. This figure shows clearly the mechanical behavior of every tissue in the vertebra: first, the cortical bone working as a bending shell is taking almost the entire load, while trabecular tissue remains practically unstressed.

Parameter	E (MPa)	ν
Trabecular bone	100	0.3
Cortical bone	12000	0.3
Alloy prosthesis and fixation system (Ti6Al4V)	110000	0.3
Polymer prosthesis (PEEK)	37000	0.3

Table 2: Material parameters adopted for the modeling.

In three-dimensional problems, the analysis in terms of principal stresses is often difficult to interpret, because at each integration point there are three values of the stresses acting in different spatial directions. Therefore, it is important to take a single representative stress value to be compared with any strength value. In the biomechanical literature, the stress state of the cortical bone is often represented by von Mises effective stress [10, 11].

Figure 4 shows the distribution of von Mises effective stress in the cortical tissue of both vertebrae in the area around the prosthesis for both polymer prosthesis (left) and for the metal alloy (right).
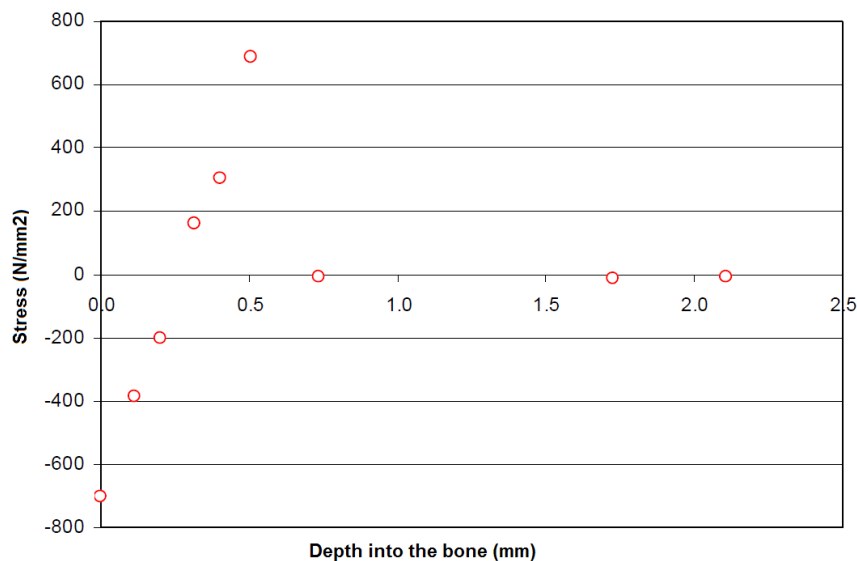
**Figure 3:** Stress distribution in the cortical and trabecular bone at a representative section.

These figures show that in both cases the maximum values are located mainly and almost exclusively in the front area of the prosthesis, with higher absolute values in the case of metallic alloy prosthesis, an expected result considering the difference between the Young's modulus of each material presented in Table 2.
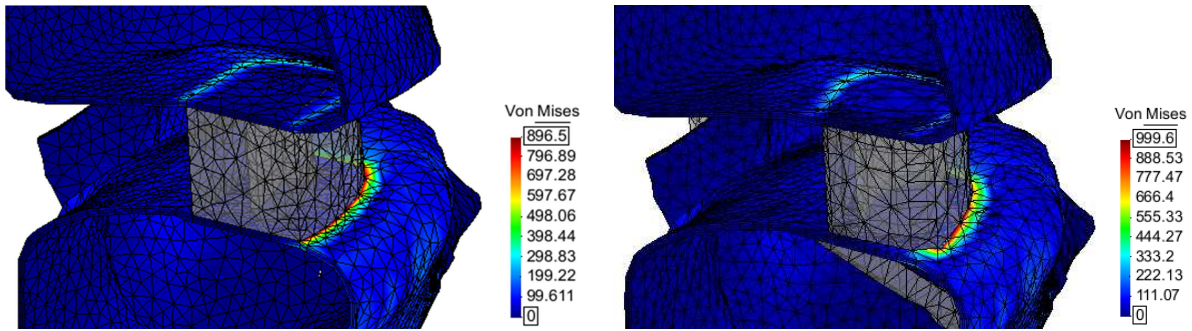
Figure 4: Effective von Mises stress (in MPa) for polymer prosthesis (left) and for metallic alloy prosthesis (right).

Figure 5 shows the same results in terms of the von Mises (left) and the HMC (right) failure criteria discussed in Section 2.4. In the figure, the zones of the cortical bone with stresses that do not reach the failure surface are represented in blue, while the zones that exceed the condition are in red. The HMC failure parameters used for this calculation are: $p = p_T = 107$ MPa [16], $\tan \varphi = 0.7$ and $C = 152$ MPa (value taken so that in pure tension the failure surface is reached in Mode I, at the vertex of the hyperboloid). These figures show that with the von Mises condition a larger number of points would be at failure if compared with the HMC condition.
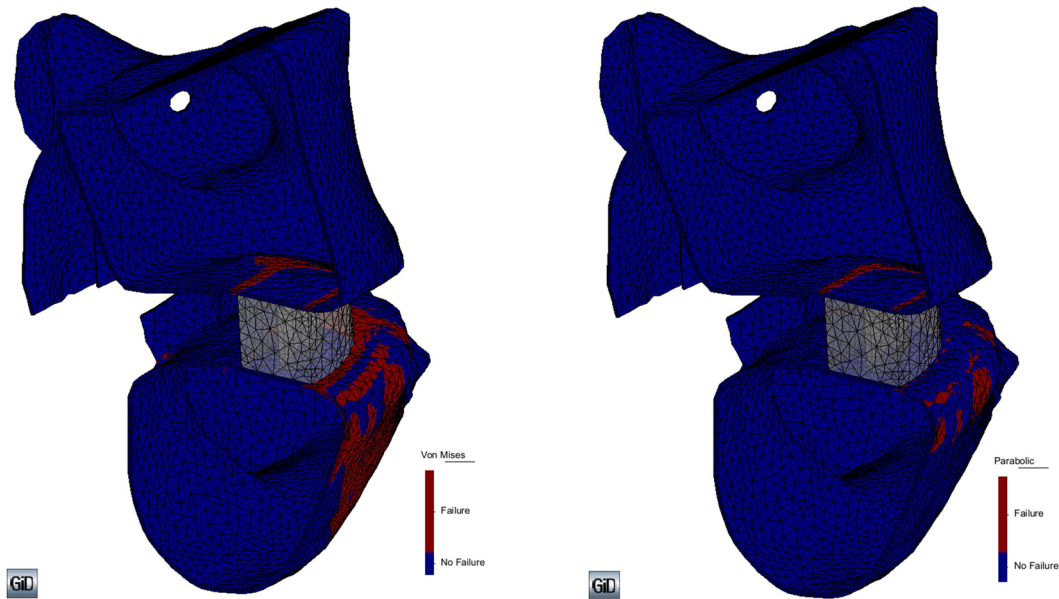
Figure 5: Graphical representation of the strength criteria of von Mises (left) and hyperbolic (right).

Figure 6 shows an additional representation of the same results in the $p - \sqrt{J_2}$ space. In the figure, the stress obtained at each Gauss point of the mesh has been represented by a dot, together with two lines which correspond to the von-Mises and HMC failure conditions. As it may be observed, a considerably greater number of Gauss points violate the von Mises criterion than the HMC criterion. In particular many points are located in the shear-

compression zone, which would be acceptable from the viewpoint of the HCM criterion (as physical for frictional mechanisms in quasi-brittle materials such as cortical bone) but not from the viewpoint of a purely deviatoric criterion such as von Mises, wich was originally developed for non-frictional materials as metals.
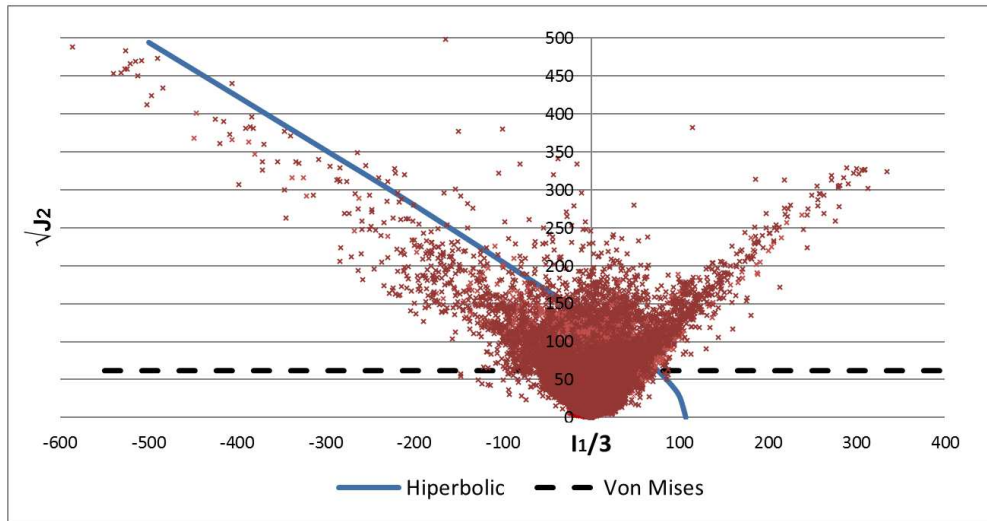
Figure 6: Graphical representation of the stress state in the $p - \sqrt{J_2}$ space for the Gauss points of the cortical tissue using polymer prosthesis (including the representation of the strength criteria of von Mises and HMC).

4 CONCLUDING REMARKS

The results obtained from the linear elastic analysis in terms of stress have shown that the mechanical behavior of the vertebra seems to be governed by the behavior of cortical tissue acting as a bending shell, while the trabecular bone underneath remains comparatively unstressed basically providing a deformable bed to the cortical bone. A comparison of the stress values with the classical von Mises strength criterion (usual in the biomechanical literature, non-frictional in nature), and with a hyperbolic Mohr-Coulomb criterion of the frictional type, shows significant differences with many more points violating the first (von-Mises) condition than the second (HCM) criterion. Note that the second should be considered much more realistic for a frictional material such as cortical bone.

Extensions of this study currently under way, include is a full nonlinear analysis using the HCM surface as the basis for an elasto-plastic constitutive model, and the consideration of the cortical bone using shell theory. The latter should provide a more rational basis for the evaluation of the vertebral cortical bone failure.

REFERENCES

[1] McAfee, P.C., Towson, M.D. Interbody fusion cages in reconstructive operations on the spine. *The journal of bone and joint surgery* 81, Number 6, pp. 859-880 (1999).

[2] Van Dijk, M., Smit, T.H., Burger, E.H., Wuisman, P.I. Bioabsorbable poli-L-lactic acid cages for lumbar interbody fusion. *Spine* 27, Number 23, pp. 2706-2714 (2002).

[3] Van Dijk, M., Smit, T.H., Arnoe, M.F., Burger, E.H., Wuisman, P.I. The use of poly-L-lactic acid in lumbar interbody cages: design and biomechanical evaluation in vitro. *Eur Spine J* 12, pp 34-40 (2003).

[4] Van Dijk, M., Smit, T.H., Sugihara, S., Burger, E.H., Wuisman, P.I. The effect of cage stiffness on the rate of lumbar interbody fusion. *Spine* 27, Number 7, pp. 682-688 (2002).

[5] Gödde, S., Fritsch, E., Dienst, M., Kohn, D. Influence of cage geometry on sagittal alignment in instrumented posterior lumbar interbody fusion. *Spine* 28, Number 15, pp. 1693-1699 (2003).

[6] Charriere, E., Sirey, F., Zysset, P.K. A finite element model of the L5-S1 functional spinal unit: Development and comparison with biomechanical tests *in vitro*. *Computer methods in biomechanics and biomedical engineering*, Vol. 6, No 4, pp. 249-261 (2003).

[7] Silva, M.J., Keaveny, T.M, Hayes, W.C. Load sharing between the shell and centrum in the lumbar vertebral body. *Spine*22, Number 2, pp. 140-150 (1997).

[8] Franzoso, G. *Analisi computazionale di un dispositivo interspinoso per la stabilizzazione di un segmento motorio del rachide lombare*. Master's thesis, Facoltà di ingegneria dei sistema, Politecnico di Milano, Milano (2004).

[9] Eberlein, R., Holzapfel, G.A., Schulze-Bauer, C.A.J. An anisotropic constitutive model for annulus tissue and enhanced finite element analyses of intact lumbar disc bodies. *Biomech Preprint Series*, paper No. 6, October (2000).

[10] Polikeit, A, Ferguson S.J., Nolte, L.P., Orr, T.E. Factors influencing stresses in the lumbar spine after the insertion of invertebral cages: finite element analysis. *Eur Spine J* 12, 413-420 (2003).

[11] Sochor, M. Experiments proposed when developing cages based on a carbon-carbon composite. *Experimental Stress Analysis*; 39th Int. Conference (2001).

[12] Pitzen, T.A. Finite element model for predicting the biomechanical behavior of the human lumbar spine. *Control Engineering Practice* 10, 83-90 (2002).

[13] Mullins, L.P., Bruzzi, M.S., McHugh, P.E. Calibration of a constitutive model for the post-yield behavior of cortical bone. *Journal of the Mechanical Behavior of Biomedical Materials* 2, 460-470 (2009).

[14] Carol, I., Prat, P.C., López, C. M. A normal/shear cracking model. Application to discrete crack analysis. *J. Engng. Mech. ASCE*, 123, pp. 765−773 (1997).

[15] Carol, I., López, C.M., Roa, O. Micromechanical analysis of quasi-brittle materials using fracture-based interface elements. *Int. J. Num. Methods in Engineering*, 52(1-2), 193-215 (2001).

[16] Cowin, S.C (Ed.). *Bone Mechanics*. CRC Press Inc. ISBN 0-8493-9117-2 (2001).